

Characteristics of nanosize spinel $\text{Ni}_{0.9}\text{Fe}_2\text{Co}_{0.1}\text{O}_4$ prepared by sol-gel method using pectin as an emulsifying agent

Septian Try Sulistiyo^a and Rudy Situmeang^b

^aGraduate student in Department of Chemistry, University of Lampung

^bDepartment of Chemistry, University of Lampung

Abstract

$\text{Ni}_{0.9}\text{Fe}_2\text{Co}_{0.1}\text{O}_4$ nanomaterial have been prepared using a sol-gel method. Preparation of material was carried out by dissolving nitrate salts of iron, cobalt and nickel, in pectin solution and then the sample was stirred throughly using magnetic stirrer while adjusting pH to 11. After freeze-drying process, the sample was subjected to calcination treatment and subsequently characterized using the techniques of X-ray diffraction (XRD), Scherrer Methods, FTIR and DT-TG analysis. The results of XRD characterization indicated that materials consist of two crystalline phases, such as CoFe_2O_4 and NiFe_2O_4 . These two crystalline phases are superimposed. DT-TGA result showed that spinel $\text{Ni}_{0.9}\text{Fe}_2\text{Co}_{0.1}\text{O}_4$ formed above 400°C . Then, PSA determination proved that the grain size of spinel ferrites is a range of 30–95.2 nm as much as 21%. Crystallite size calculation using Scherrer equation, proved that the size is 31.95 nm. Its size increased as temperature calcination augmented.

Keywords Nanomaterial, spinel ferrites, Brønsted–Lowry and Lewis acid sites, freeze-drying

1. Introduction

Spinel structured materials have an interesting physical and chemical characteristics therefore these materials have been utilized abroadly in industrial applications such as catalysts (Van der Laan & Beenackers, 1999; Rajput & Kaur, 2013; Mangrulkar et al., 2012), memory devices (Lu et al., 2007], sensors (Abdel-Latif, 2012; Tudorache & Petrila, 2013], magnetic materials (Mukherjee & Mitra, 2014; Shokrollahi & Sharifi, 2013) and materials for stealth technology (Pullar, 2012; Zhao et al., 2009). This interesting both chemical and physical properties is determined mainly by the occupations of cations at both octahedral and tetrahedral sites in the spinel ferrites, $\text{M}_1\text{M}_2\text{Fe}_2\text{O}_4$ where M_1 and M_2 are +2 or +3 cations, and M_1 or M_2 could be Co^{+2} , Ni^{+2} , Cu^{+2} , Zn^{+2} , Mo^{+3} and others (El-Sayed, 2003; Juang & Mathew, 2007). One of the other factors determining its performance on the application is the method of preparation.

Preparation methods that have been used currently to produce spinel ferrites are coprecipitation (Murthy et al., 2009; Derakhshi et al., 2012), sol-gel (Singhal et al., 2005; Trisunaryanti et al., 2008), soft mechanochemical (Lazrević et al., 2012), hydrothermal (Nejati & Rezvanh, 2012; Zhou et al., 2005) and precipitation (Yang et al., 1999; Yongvanich et al., 2010; Atashi et al., 2013). The aim of those preparations is to devote and focus on two aspects e.g development of synthetic method and development of various materials which satisfy the continuous growing of utilization.

In the present experimental work, we focused on obtaining nano ferrites particles and examining the effect of temperature calcination. The synthesis of spinel nickel cobalt ferrite nano-material has been prepared by sol-gel method using pectin as an emulsifying agent at

low temperature. The phases developed for nano-material is identified qualitatively by XRD analysis. Microstructural size is determined by Particle Size Analyzer and Scherrer equation. Then, FTIR analysis is done successively to confirm the bond formation and acid sites of those nano materials .

2. Materials and methods

2.1 Materials

Materials used in this work are pectin powder, $\text{Ni}(\text{NO}_3)_2 \cdot 6\text{H}_2\text{O}$ (Merck, 99%), $\text{Fe}(\text{NO}_3)_3 \cdot 9\text{H}_2\text{O}$ (Merck, 99%), $\text{Co}(\text{NO}_3)_2 \cdot 6\text{H}_2\text{O}$ (Merck, 99%), pyridine ($\text{C}_5\text{H}_5\text{N}$, J.T Baker), NH_3 (Merck, 99%), and aquades.

2.2 Instrumentations

The instruments used for characterization were Fourier Transform Infrared (FTIR) spectrometer (Shimadzu Prestige-21) for identifying the presence of functional groups, and Differential Temperature and Gravimetry analysis (DT-GA) for elucidating the formation process . Then, a Philips X-ray diffractometer (XRD) model PW 1710 with $\text{Cu-K}\alpha$ radiation was used for structural and crystalline phases identification.

2.3 Preparation of $\text{Ni}_{0.9}\text{Fe}_2\text{Co}_{0.1}\text{O}_4$ nanomaterial

Stoichiometric amount of Ni (II) nitrate hydrates, Co (II) nitrate hydrates and Fe (III) nitrate hydrates were dissolve in distilled water, having compositions $\text{Ni}_{0.9}\text{Fe}_2\text{Co}_{0.1}\text{O}_4$ under magnetic stirring for 1 hour, respectively, followed by mixing each solution to make final solution molar ratio between nitrates to pectin is 3:2. Adjust the $\text{pH}=11$ in the above solution by addition of ammonia, and heat it at 80°C with continue stirring to form viscous gel. Dried the gel using freeze dryer for 7 hours to form the precursors' networks and calcined at 600 and 800°C for 3hours. Finally Co doped Ni - ferrite nanoparticles has prepared.

2.4 Characterization of $\text{Ni}_{0.9}\text{Fe}_2\text{Co}_{0.1}\text{O}_4$ nanomaterial

Differential temperature and gravimetry analysis

Sample of approximately 5–6 mg precursor was placed in Pt-sample pan and another pan was allowed blank as a reference. The experiment was carried out under a flowing nitrogen atmosphere (50 ml/min, SII TG/DTA 7300). Then, scan analysis was worked in the range of 25 to 600°C with a heating rate of 5°C min^{-1} .

X- ray diffractogram analysis

X-ray powder diffraction pattern of the sample was recorded from $2\theta = 10$ to 90° on a Philips diffractometer Model PW 1710 using $\text{Cu K}\alpha$ radiation at a step 0.02° per second. The phase identification was performed using search and match method by comparing the x-ray pattern of the sample to those of the standards in the COD using Phase Identification from Powder Diffraction Files, and identified phase was quantified using Rietveld method (Rietveld, 1969). The particle size was also determined using Debye–Scherrer method (Cullity, 1978).

Acid sites analysis of $\text{Ni}_{0.9}\text{Fe}_2\text{Co}_{0.1}\text{O}_4$

After heating at 120°C , sample was transferred into a crucible and placed in vacuumized dessicator. Pyridine was transferred into another crucible and placed in the dessicator to allow the vapour of the pyridine to contact with the sample. After 24 hours, the sample was taken from dessicator and left on open air for 2 hours to expell the physically adsorbed pyridine from the sample. Finally, the sample was analyzed using the FTIR spectroscopy. The analysis was conducted by grinding the sample with KBr of spectroscopy grade, and scanned over the wave number range of $4000 - 400 \text{ cm}^{-1}$ (Parry, 1963; Ryczkowski, 2001).

3. Results and discussion

Differential temperature and gravimetry analysis

The precursor of $\text{Ni}_{0.9}\text{Fe}_2\text{Co}_{0.1}\text{O}_4$ nanomaterial prepared were characterized using thermal analysis techniques such as differential temperature and thermal gravimetric analysis (DT-TGA). Thermal gravimetric analysis was used to measure the losses of weight as a function of temperature. The TGA results for the 4.8 h aged precursor containing $[\text{Ni}]/[\text{Co}] = 9/1$ molar ratio is shown in Figure 1.

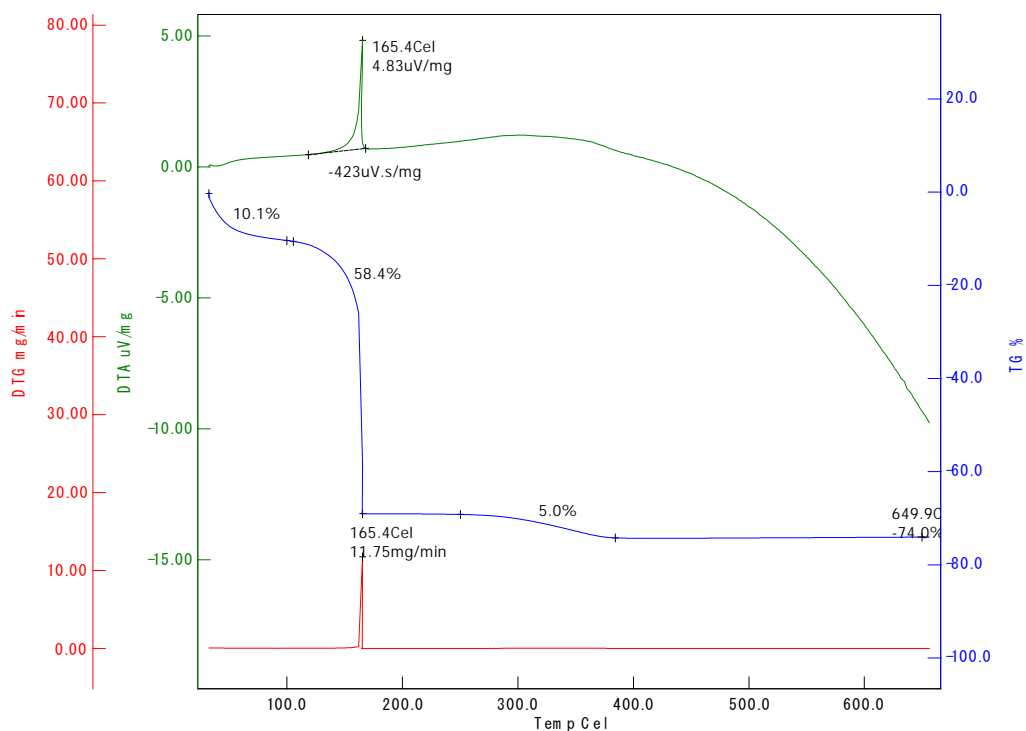


Figure 1. DT-TGA curve for $\text{Ni}_{0.9}\text{Fe}_2\text{Co}_{0.1}\text{O}_4$ nanomaterial precursor with $\text{Ni} / \text{Co} = 9/1$ molar ratio

There is a gradual weight loss upon heating to about 200°C ; above this temperature there is a crucial weight loss until 400°C . During the first period of the weight loss, the exothermic process is occurred at 165.5°C and the energy of $4.83 \mu\text{V}/\text{mg}$. The first weight loss with temperatures range of $80-200^\circ\text{C}$ and is due to the removal of absorbed water in pectin networks. The second period of weight losses with temperatures at around $200-400^\circ\text{C}$, are

considered to be due to the decomposition of pectin, and nitrate precursors, so that the decomposition at these high temperature regions produce water, carbon dioxides and nitrogen oxides simultaneously. Above 400°C, there is no weight loss and the formation of $\text{Ni}_{0.9}\text{Fe}_2\text{Co}_{0.1}\text{O}_4$ nanomaterial is started.

X-ray diffractogram analysis

The prepared sample was characterized by Philips PW-1710 X-ray diffractometer using Cu-K α radiation ($\lambda = 1.5406 \text{ \AA}$) source. The X-ray diffraction patterns of the prepared sample is shown in Figure 2.

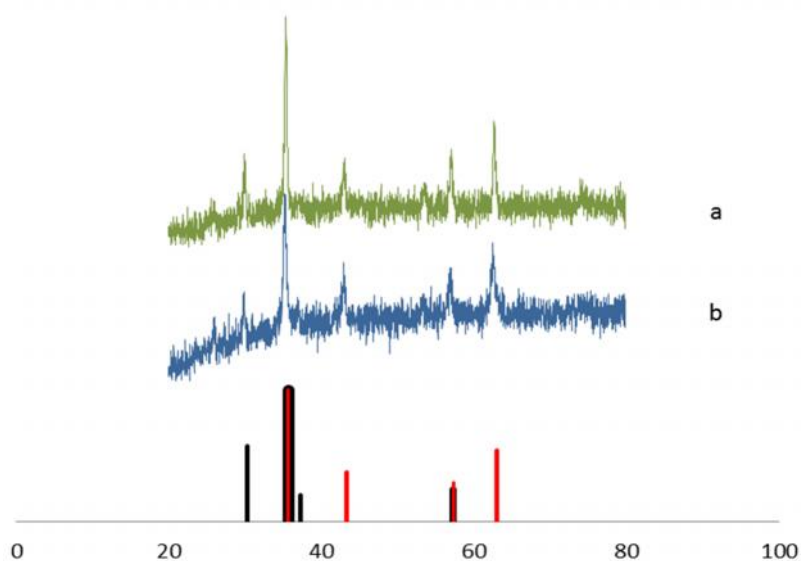


Figure 2. Diffractogram of $\text{Ni}_{0.9}\text{Fe}_2\text{Co}_{0.1}\text{O}_4$ nanomaterial after calcining at: (a) 800°C and (b) 600°C. (Notes: black bar-peaks refers to CoFe_2O_4 and red bar-peaks refers to NiFe_2O_4)

The diffraction pattern of $\text{Ni}_{0.9}\text{Fe}_2\text{Co}_{0.1}\text{O}_4$ together with some standards related to the predicted phases of the sample was presented in Figure 2. With the aid of search and match method, using Phase Identification from Powder Diffraction Files, it was found that the major phase is spinel NiFe_2O_4 (JCPDF- 10-0325), CoFe_2O_4 (JCPDF-22-1086). In general, it can be implied that both NiFe_2O_4 and CoFe_2O_4 crystalline phases are superimposed. By increasing calcination temperature, the formation of spinel compounds is more pronounced as shown in Figure 2 above. The peaks of spinel compound were shifted a little bit to references' peak pattern (bar - peaks).

Moreover, the crystallite size of $\text{Ni}_{0.9}\text{Fe}_2\text{Co}_{0.1}\text{O}_4$ nanomaterial was calculated from the most prominent peak (211) of XRD using the Scherer formula (Cullity, 1978):

$$D = \frac{k \lambda}{\beta \cos \theta}$$

where D is the crystallite size (nm), $\lambda = 1.5406 \text{ \AA}$ or 0.15406 nm is the wavelength of incident X-ray, θ is the diffraction angle at the prominent peak and β is the broadening of diffraction line measured at half maximum intensity, $\frac{f}{1} \times F$ (in radian), and k is a constant with range of 0.9–1.0 (in this calculation, $k = 0.94$). θ is the Bragg's angle in degree unit. The calculation results are compiled in Table 1.

As shown in Table 1, the crystallite sizes of $\text{Ni}_{0.9}\text{Fe}_2\text{Co}_{0.1}\text{O}_4$ samples are in the range of 11–21 nm, demonstrating the efficacy of the proposed method to produce nano-size spinel $\text{Ni}_{0.9}\text{Fe}_2\text{Co}_{0.1}\text{O}_4$. In relation with the calcination variation, it was found that the higher the calcination temperature used the larger the crystallite size formed.

Table 1. Crystallite size calculation using Scherrer equation

$\text{Ni}_{0.9}\text{Fe}_2\text{Co}_{0.1}\text{O}_4$ Calcined at	2 θ , deg	hkl	FWHM		Size of Crystallite (D), nm
			degree	(β)/ radian	
600°C	35.16	211	0.7510	0.013113	11.58
800°C	35.32	211	0.4265	0.007974	20.41

Acid sites analysis of $\text{Ni}_{0.9}\text{Fe}_2\text{Co}_{0.1}\text{O}_4$

Fourier transform infrared spectroscopy was applied to identify the functional groups present in the sample, primarily to identify the existence of Lewis and Brønsted–Lowry acid sites. The acid sites identification is of particular importance since the acidity is acknowledged as very important characteristic which determine the performance of a material as a catalyst (Parry, 1963; Ryzkowski, 2001). The FTIR spectra of $\text{Ni}_{0.9}\text{Fe}_2\text{Co}_{0.1}\text{O}_4$ sample investigated is shown in Figure 3.

As shown in Figure 3, In general, the peaks appeared at the wavelength range of 3500–3000 cm^{-1} are assigned to O-H stretching vibration, and the absorption bands located at 630–580 cm^{-1} and at 480–420 cm^{-1} are assigned to strong and weak stretching vibrations of M-O modes, respectively (Parry, 1963; Ryzkowski, 2001; Yurdakoç et al., 1999). The presence of M-O modes is supported by the vibration band located at the wavelength of 570–560 cm^{-1} . The existence of Brønsted–Lowry and Lewis sites is displayed by the absorption bands located at 1475–1420 cm^{-1} and 1620–1510 cm^{-1} , respectively (Yurdakoç et al., 1999; Boucheffa et al., 2008).

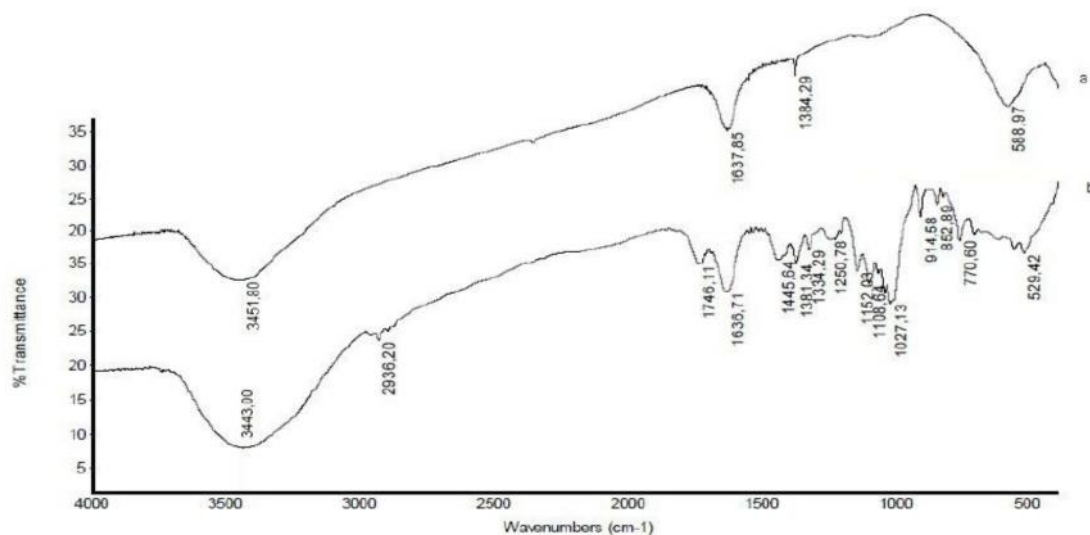


Figure 3. FTIR Spectrum of $\text{Ni}_{0.9}\text{Fe}_2\text{Co}_{0.1}\text{O}_4$ after exposed to pyridine vapour: (a) calcined at 600°C and (b) calcined at 800°C.

In the samples investigated, calcined at 600 and 800°C, the presence of O-H functional group is indicated by the absorption band, resulted from stretching vibration, located at

3451.80 and 3443.00 cm^{-1} , respectively. The existence of Lewis acid sites in the sample calcined at 800°C is displayed by the adsorption bands located at 1746.11 and 1636.71 cm^{-1} which indicate that the pyridine was bound to the surface of the sample by coordination bond [Parry, 1963] and more pronounced than that of calcined at 600 °C, while the existence of Brønsted–Lowry acid sites is presented by the absorption bands located at 1445.64 and 1381.34 cm^{-1} for the sample calcined at 800°C and 1384.29 cm^{-1} for the sample calcined at 600 °C. By comparing the intensities of the absorption bands associated with Lewis and Brønsted–Lowry acid sites, it can be concluded that the acid characteristic of the sample is dominated by Lewis acid. In the fingerprint region of the spectra, the absorption band representing stretching vibration of Fe-O and bending vibration of Ni-O and Co-O was detected at 588.97, 529.42 and 440 cm^{-1} [Ryckowski, 2001], suggesting the existences of Fe-O-Ni and Fe-O-Co bond which confirms the formation of $\text{Ni}_{0.9}\text{Fe}_2\text{Co}_{0.1}\text{O}_4$ structure as expected. In addition, the peaks appeared which are displayed by the absorption bands located in the range of 914.58–770 cm^{-1} refers to the possibility of metal-metal bond formation.

4. Conclusion and remarks

This current study demonstrated the potential of pectin solution as a emulsifying agent for preparation of nano-size materials using sol-gel method. The XRD results revealed that the crystallite size of the $\text{Ni}_{0.9}\text{Fe}_2\text{Co}_{0.1}\text{O}_4$ sample prepared is in the range of 11 to 21 nm. The samples were found to exhibit Lewis and Brønsted–Lowry acid characteristics, with Lewis acid as the dominant site, as revealed by the FTIR analyses.

Acknowledgment

The authors wish to thank and appreciate the Directorate General Higher Education Republic of Indonesia for research funding provided through The National Grant for Competitive Research University of Lampung and Ministry of Indonesia Higher Education Program.

References

- Abdel-Latif, I.A. (2012). Fabrication of nano-size nickel ferrites for gas sensors applications. *J. Phys.*, 1(2), 50–53.
- Atashi, H., Sarkaria, M., Fazlollahib, F., Mirzaeid, A.A., & Heckerb, W.C. (2013). Using different preparation methods to enhance Fischer–Tropsch Products over iron-based catalyst. *Chem. Biochem. Eng. Q.*, 27(3), 259–266.
- Boucheffa, Y., Benaliouche, F., Ayrault, P., Mignard, S., & Magnoux, P. (2008). NH_3 -TPD and FTIR spectroscopy of pyridine adsorption studies for characterization of Ag- and Cu- exchanged X-zeolites. *Microporous and Macroporous Material*, 113(1–3), 80–88.
- Cullity, B.D. (1978). *Elements of X-ray diffraction* (2nd ed.). Addison-Wesley, London.
- Derakhshi, P., Khorrami, S.A., & Lotfi, R. (2012). An Investigation on synthesis and morphology of nickel doped cobalt ferrite in the presence of surfactant in different calcination temperature by coprecipitation route. *World Appl. Scie. J.*, 16(2), 156–159.
- El-Sayed, A.M. (2003). Electrical conductivity of nickel–zinc and Cr substituted nickel–zinc ferrites. *Mat. Chem. Phys.*, 82, 583–587.
- Juang, R.-S., & Mathew, D.S. (2007). An overview of the structure and magnetism of spinel ferrite nanoparticles and their synthesis in microemulsions. *Chem. Eng. J.*, 129(1–3), 51–65.

- Lazrević, Z.Ž., Jovalekić, Č., Milutinović, A., Romčević, M.J., & Romčević, N.Ž. (2012). Preparation and characterization of nano ferrites. *Acta Physica Polonica A*, 121(3), 682–686.
- Mangrulkar, P.A., Polshettiwar, V., Labhsetwar, N.K., Varma, R.S., & Rayalu, S.S. (2012). Nano-ferrites for water splitting: unprecedented high photocatalytic hydrogen production under visible light. *Nanoscale*, 4(16), 5202–5209.
- Mukherjee, S., & Mitra, M.K. (2014). Characterization of perovskite-spinel nanocomposites (BFO-ZFO) ferrites prepared by chemical route. *J. Austr. Ceram. Soc.*, 50(2), 180–187.
- Murthy, Y.L.N., Viswanath, I.V.K., Rao, T.K., & Singh, R. (2009). Synthesis and characterization of nickel copper ferrite. *Int. J. ChemTech Research*, 1(4), 1308–1311.
- Nejati, K., & Zabihi, R. (2012). Preparation and magnetic properties of nano size nickel ferrite particles using hydrothermal method. *Chem. Centr. J.*, 6, 23.
- Parry, E.P. (1963). An Infrared study of pyridine adsorbed on acidic solids characterization of surface acidity. *J. Catal.*, 2(5), 371–379.
- Pullar, R.C. (2012). Hexagonal ferrites: A review of the synthesis, properties and applications of hexaferrite ceramics. *Prog. Mater Sci.*, 57(7), 1191–1334.
- Rajput, J.K., & Kaur, G. (2013). CoFe_2O_4 nanoparticles: An efficient heterogeneous magnetically separable catalyst for “click” synthesis of arylidene barbituric acid derivatives at room temperature. *Chin. J. Catal.*, 34, 1697–1704.
- Ryczkowski, J. (2001). IR spectroscopy in catalysis. *Catalysis Today*, 68, 263–381.
- Singhal S., Singh, J., Barthwal, S.K., & Chandra, K. (2005). Preparation and characterization of nanosize nickel-substituted cobalt ferrites ($\text{Co}_{1-x}\text{Ni}_x\text{Fe}_2\text{O}_4$). *J. Sol. Stat. Chem.*, 178(10), 3183–3189.
- Shokrollahi, H., & Sharifi, I. (2013). Structural, magnetic and mossbauer evaluation of Mn substituted Co–Zn ferrite nanoparticles synthesized by co-precipitation. *J. Magn. Magn. Mat.*, 334, 36–40.
- Trisunaryanti, W., & Oktaviano, H.S. (2008). Sol–gel derived Co and Ni based catalysts: Application for steam reforming of ethanol. *Indo. J. Chem.*, 8(1), 47–53.
- Tudorache, F., & Petrila, I. (2013). Humidity sensor applicative material based on copper-zinc-tungsten spinel ferrite. *Mater. Lett.*, 108, 129–133.
- Valenzuela, R., Cruz-Franco, B., Gaudisson, T., Ammar, S., Bolarín-Miró, A.M., Mazaleyra, F., Nowak, S., Vázquez-Victorio, G., Ortega-Zempoalteca, R., & de Jesús, F.S. (2014). Magnetic properties of nanostructured spinel ferrites. *IEEE Trans. on Magn.*, 50(4), 280–286.
- Van der Laan, G.P., and Beenackers, A.A.C.M. (1999). Kinetics and selectivity of the Fischer–Tropsch synthesis: A literature review. *Catal. Rev.: Sci. Eng.*, 41(3–4), 255–318.
- Yang, J.M., Tsuo, W.J., & Yen, F.S. (1999). Preparation of ultrafine nickel ferrite powders using mixed Ni and Fe Tartrates. *J. Solid State Chem.*, 145(1), 50–57.
- Yongvanich, N., Visuttipitukkul, P., Leksuma, P., Vutcharaammat, V., & Sangwanpant, P. (2010). Sinterability and microstructure of bi-added SnO_2 nanomaterials by precipitation method. *Journal of Metals, Materials and Minerals*, 20(3), 67–72.
- Yurdakoç, M., Akçay, M., Tonbul, Y., & Yurdakoç, K. (1999). Acidity of silica-alumina catalysts by amine titration using Hammett indicators and FT-IR study of pyridine adsorption. *Turk. J. Chem.*, 23, 319–327.
- Zhao, D.-L., Lv, Q., & Shen, Z.-M. (2009). Fabrication and microwave absorbing properties of Ni–Zn spinel ferrites. *Journal of Alloys and Compounds*, 480(2), 634–638.
- Zhou, J., Ma, J., Sun, C., Xie, L., Zhao, Z., Tian, H., Wang, Y., Tao, J., & Zhu, X. (2005). Low-temperature synthesis of NiFe_2O_4 by a hydrothermal method. *Journal of the Am. Cer. Soc.*, 88(12), 3535–3537.